Original Research

Contusion concomitant with ischemia injury aggravates skeletal muscle necrosis and hinders muscle functional recovery

Peijun Deng[1,2,3,4], Shuai Qiu[1,2,3,4], Fawei Liao[1,2,3,4], Yifei Jiang[1,2,3,4], Canbin Zheng[1,2,3,4] and Qingtang Zhu[1,2,3,4]

[1]Department of Microsurgery, Orthopedic Trauma and Hand Surgery, First Affiliated Hospital, Sun Yat-sen University, Guangzhou 510080, China; [2]Guangdong Province Engineering Laboratory for Soft Tissue Biofabrication, Guangzhou 510080, China; [3]Guangdong Provincial Peripheral Nerve Tissue Engineering and Technology Research Center, Guangzhou 510080, China; [4]Guangdong Provincial Key Laboratory of Orthopaedics and Traumatology, Guangzhou 510080, China
Corresponding authors: Canbin Zheng. Email: zhengcb3@mail.sysu.edu.cn; Qingtang Zhu. Email: zhuqingt@mail.sysu.edu.cn

Impact Statement

Contusion concomitant with ischemia injury to skeletal muscle always leads to disability in limbs and remains a great challenge to be treated. Unfortunately, the alterations that occur in skeletal muscle after contusion concomitant with ischemia injury remain unclear. This study demonstrated that compared with contusion injury or ischemia injury alone, contusion concomitant with ischemia injury to skeletal muscle not only aggravates early muscle fiber necrosis but also hinders muscle functional recovery by impairing satellite cell differentiation and exacerbating fibrosis during skeletal muscle repair. This finding improves our understanding of the pathological and functional alterations in skeletal muscle after contusion concomitant with ischemia injury. Furthermore, it provides insight into the mechanism of muscle regeneration disorders caused by this type of injury. Moreover, these findings can arouse surgeons' attention to promoting the management of this type of injury.

Abstract

Contusion concomitant with ischemia injury to skeletal muscles is common in civilian and battlefield trauma. Despite their clinical importance, few experimental studies on these injuries are reported. The present study established a rat skeletal muscle contusion concomitant with ischemia injury model to identify skeletal muscle alterations compared with contusion injury or ischemia injury. Macroscopic and microscopic morphological evaluation showed that contusion concomitant with ischemia injury aggravated muscle edema and hematoxylin–eosin (HE) injury score at 24 h postinjury. Serum creatine kinase (CK) and lactate dehydrogenase (LDH) levels, together with gastrocnemius muscle (GM) tumor necrosis factor-alpha (TNF-α) content elevated at 24 h postinjury too. During the 28-day follow-up, electrophysiological and contractile impairment was more severe in the contusion concomitant with ischemia injury group. In addition, contusion concomitant with ischemia injury decreased the percentage of larger (600–3000 μm^2) fibers and increased the fibrotic area and collagen I proportion in the GM. Smaller proportions of $Pax7^+$ and $MyoD^+$ satellite cells (SCs) were observed in the contusion concomitant with ischemia injury group at 7 days postinjury. In conclusion, contusion concomitant with ischemia injury to skeletal muscle not only aggravates early muscle fiber necrosis but also hinders muscle functional recovery by impairing SC differentiation and exacerbating fibrosis during skeletal muscle repair.

Keywords: Skeletal muscle, contusion, ischemia, inflammation, muscle regeneration, satellite cell

***Experimental Biology and Medicine* 2022; 247: 1577–1590. DOI: 10.1177/15353702221102376**

Introduction

Skeletal muscle is widely distributed and superficially located throughout the body, making it vulnerable to injury in daily life.[1] Among the various types of injuries, contusion injuries are common in the fields of traumatology, orthopedics, and sports medicine.[2] They are mainly caused by acute, relatively high-energy blunt trauma and are characterized by myofiber rupture and secondary injuries, such as inflammation and fibrosis.[3] Skeletal muscle has a remarkable ability to repair itself following contusion injury. The repair process is complex but well understood, which consists of overlapping phases of degeneration, inflammation, regeneration, and fibrosis.[4,5] Ischemia injury is another common type of injury to skeletal muscle. Skeletal muscle has high metabolic activity and therefore is acutely sensitive to a decrease in blood supply.[6] Ischemia in skeletal muscle leads to energy depletion, accumulation of toxic metabolic products, activation of phospholipase and lysozymes, and cell damage.[7] Furthermore, reperfusion after ischemia causes more extensive damage through oxidative stress, neutrophil infiltration, and inflammation.[8,9] Following ischemia injury, skeletal muscle can be repaired itself, similar to after contusion injury.[10]

In the clinic, a large number of patients experience contusion and ischemia injury to skeletal muscle simultaneously, such as in the case of Gustilo type III open fracture, blunt arterial injury, acute compartment syndrome, and tourniquet application during traumatic limb surgery.[11,12] In these situations, progressive muscle necrosis requires multiple debridements in the early treatment. After that, self-repair process is initiated. Although skeletal muscle has a remarkable self-repair ability, insufficient regeneration and fibrosis are inevitable, leading to chronic muscle pain, disability, and secondary amputation. It is of great challenge in managing patients with contusion concomitant with ischemia injury to skeletal muscle. However, alterations of skeletal muscle after contusion concomitant with ischemia injury have not been revealed clearly. This study aimed to establish a rat skeletal muscle contusion concomitant with ischemia injury model to identify skeletal muscle alterations and mechanism compared with contusion injury or ischemia injury.

Materials and methods

Animals and model

A total of 135 male Sprague–Dawley (SD) rats (weighing 200–220 g) from the Central Animal Facility of Sun Yat-sun University were used in this study. All the animals were housed in appropriate cages at a temperature of 22 ± 2°C and a relative humidity of 40–60% on a 12-h light–dark cycle with free access to food and water. All experimental protocols were approved by the Animal Experimentation Ethics Committee of First Affiliated Hospital of Sun Yat-sen University (approval no. SYSU-IACUC-2020-000548). After being acclimatized for 7 days, the rats were randomly allocated into three groups. The right hindlimb was injured, and the left hindlimb was used as a control. The rats were anesthetized by intraperitoneal (i.p.) injection of pentobarbital (40 mg/kg). After the rats were totally anesthetized, the right lower limb was shaved and used for modeling.

In the contusion injury group (group C), a contusion model was established using a self-designed drop-mass device as described previously.[13,14] Briefly, the right hind leg of each rat was fixed so that the knee was extended and the ankle was dorsiflexed to 90°. A weight with a diameter of 38 mm (500 g) was dropped from a height of 35 cm through a PVC tube with an interior diameter of 38.1 mm onto an impactor with a surface area of 0.785 cm^2 that rested on the medial surface of the gastrocnemius muscle (GM). In the pilot study, a hematoma developed immediately in the impacted area of the GM, but no fracture or vascular injury was detected in the injured leg. In the ischemia injury group (group I), an ischemia model was established by applying an elastic rubber band above the right greater trochanter as described previously.[15,16] Two hours later, the elastic rubber band was removed. In the contusion concomitant with ischemia injury group (group C + I), the animals were subjected to GM contusion (as described for group C) followed by hindlimb ischemia (as described for group I).

After injury, the rats were transferred to clean cages and given free access to food and water. For further analysis, the rats were anesthetized as described above or sacrificed by overdose of pentobarbital.

Muscle edema

The extent of GM edema was determined by measuring the wet-to-dry weight ratio. At 24 h postinjury, five rats from each group were sacrificed, and the GMs were harvested and weighed (wet weight). Then, the GM tissues were dried for 48 h in a laboratory oven at 55°C and weighed again (dry weight) to calculate the wet-to-dry weight ratio.

Triphenyl tetrazolium chloride assay

Triphenyl tetrazolium chloride (TTC) staining was performed to detect the ischemic infarct in the GM as described previously.[17] At 24 h postinjury, rats from each group ($n = 5$) were sacrificed, and the GMs were harvested. After the adherent fascia, fat, and tendons were removed, the muscles were cut into 2 mm transverse slices and washed with cold normal saline to eliminate any blood. The slices were blotted dry with paper towels and incubated in 2% TTC (Servicebio, Wuhan, China) at 37°C in the dark for 30 min for staining and photographed. Viable skeletal muscle and infarcted muscle were stained in different colors. The infarct size in each slice was calculated using ImageJ software (ImageJ, MD, USA) and summed. Ratios of infarct area to the total area of the muscle were calculated.

Histology and morphometric analysis

Rats ($n = 5$) were sacrificed at different time points after injury (1, 7, 14, and 28 days), and the right GM was harvested. The GM tissues were fixed with 4% paraformaldehyde for 24 h and then embedded in paraffin, specimens were cut into 10 μm transects using a microtome (Leica EG 1160, Germany). Then, the sections were deparaffinized, hydrated, and stained with hematoxylin–eosin (HE) (Jiancheng, Nanjing, China), and Masson trichrome (Biosharp, Hefei, China). Images of each muscle section were captured using a 20× objective (Labophot 2, Nikon, Tokyo, Japan). The fourfold divided frame counting method was used to assess HE staining and determine the muscle injury score at 24 h postinjury as described previously.[18] In brief, each image was divided into 15 fields that covered the entire cross-section of the muscle. Then, each field was split into four equal sections, and a random number generator was used to determine the order in which the quadrants of the field were scored. Myocytes were scored as uninjured or injured based on individual morphology by two experimenters in a blinded and independent manner. The muscle injury score is expressed as a percentage and was calculated by dividing the number of injured myocytes by the total number of myocytes in all slides. To analyze Masson trichrome staining, five 2000 × 2000 μm fields were randomly selected from each slice as the region of interest (ROI). Muscle fiber cross-sectional areas (CSAs) in each ROI were manually measured using ImageJ software (ImageJ, MD, USA). Fiber size distributions were further analyzed in each group with a 600 μm^2 bin width as previously described.[19,20] The percentage of collagen fiber area relative to the total area was calculated using ImageJ software (ImageJ, MD, USA) too.

Laboratory measurements

The serum creatine kinase (CK) and lactate dehydrogenase (LDH) levels of each rat were measured 24 h postinjury.

In brief, blood samples were collected by cardiac puncture. After centrifugation (2 × 10 min, 1500 rpm), the serum samples were snap-frozen in liquid nitrogen and stored at −80°C until they were analyzed with an automatic chemistry analyzer (Chemray 800, Rayto, Shenzhen, China). The content of tumor necrosis factor-alpha (TNF-α) in muscle was measured at a wavelength of 450 nm using an ELISA kit according to the manufacturer's instructions (ml002859, Enzyme-linked, Shanghai, China).

Electrophysiological assessment

At different time points after injury (1 and 28 days), animals ($n = 5$) were randomly selected from each group and anesthetized. The sciatic nerves and GM were partially exposed. A stimulating bipolar electrode was applied to the nerve trunk, and data were recorded from the ipsilateral GM belly using an EMG recorder (BL-420F, TaiMeng, Chengdu, China). The compound muscle action potential (CMAP) amplitude was recorded. This experiment was repeated five times. A pilot study was used to determine the optimal electrical stimulation settings before measurement. The stimulus intensity was set to 2.0 V, and the duration was set to 0.01 ms.

Muscle contractility test

After electrophysiological assessment, a muscle contractility test was performed. The proximal GM belly and distal Achilles tendon were exposed, and the middle portion of the GM was kept under the skin to prevent cooling and desiccation. The Achilles tendon was cut at the ankle, and a 4-0 silk anchoring the distal tendon of the muscle was tied to a force transducer (FT-102, TaiMeng, Chengdu, China). The force transducer signal was processed using Labscribe software (TaiMeng, Chengdu, China). The anchoring silk was positioned, so that, the GM was in a position similar to its anatomical position. Stimulation was accomplished via two needle electrodes placed transversely across the bulk of the GM fibers proximally within the GM belly. A pilot study was used to determine the optimal electrical stimulation settings before measurement. For twitch force measurement, the optimal electrical stimulus intensity was set to 2 V, and the duration was set to 0.01 ms. For tetanic force measurement, the stimulus intensity was set to 10 V, the pulse duration was set to 2 ms, and the pulse frequency was set to 35 Hz. Equal settings were used for all stimulating pulses in all measurements. The GMs were rested for 1 min between stimulations with no preload to avoid muscle fatigue. Force measurements were displayed digitally, and the maximum value of five measurements was obtained using Labscribe software (TaiMeng, Chengdu, China).

Collagen analysis

Slides collected at 28 days postinjury were stained with Sirius Red (Servicebio, Wuhan, China) as described in previous publications. After staining, each slide was imaged using a Nikon Eclipse E100 microscope (Nikon, Tokyo, Japan) with a ×10 objective and a Nikon DS-U3 camera (Nikon, Tokyo, Japan) under polarized light, and the entire cross-section was reconstructed by merging the images using Photoshop. Collagen I and collagen III were identified as red-orange and green fibers, respectively, and ImageJ software (ImageJ, MD, USA States) was used to calculate the areas of collagen fibers.

Immunohistochemistry

The GMs of rats in each group were harvested at 7 days postinjury for immunofluorescence staining. After being fixed with 4% paraformaldehyde for 24 h and dehydrated in 30% sucrose solution for 48 h at room temperature, the GM muscles were cut into 10 μm transverse sections with a cryostat (Thermo NX50) and stored at −80°C. The slides were washed in phosphate-buffered saline (PBS) for 5 min and then immersed in blocking solution (10% normal goat serum in PBS and 0.5% Triton X-100) for 1 h and then incubated with primary antibody (paired box protein 7 (Pax7), 1:20, supernatant, Developmental Studies Hybridoma Bank; myogenic determination protein (MyoD), 1:100, sc-377460, Santa Cruz; laminin, 1:400, L9393, Sigma-Aldrich) at 4°C overnight. After being washed three times for 5 min in PBS, the slides were incubated with secondary antibodies (Alexa Fluor 594-conjugated goat anti-mouse IgG, 1:500, A11005, Invitrogen; Alexa Fluor 488-conjugated goat anti-rabbit IgG, 1:500, A11008, Invitrogen) for 1 h and then washed three times for 5 min each in PBS. Finally, the slides were incubated with DAPI (2-(4-Amidinophenyl)-6-indolecarbamidine dihydrochloride 1:1000, C1002, Beyotime) for 10 min, washed three times for 5 min each in PBS, and mounted with mounting solution (AR-0851, Dingguo). The number of $Pax7^+$ and $MyoD^+$ cells in five high-power fields (HPF, 200× magnification) per slide from five rats in each group was counted.

Statistical methods

Statistical analysis was performed using GraphPad Prism 8.0 (GraphPad Software, San Diego, USA). The Kolmogorov–Smirnov normality test and Brown–Forsythe test were used to determine whether the quantitative data were normally distributed and whether the standard deviations were significantly different, respectively. The data are presented as the means ± standard deviation. Significance was typically analyzed by paired *t*-test, one-way analysis of variance (ANOVA), and two-way ANOVA followed by the post hoc Least—Significant Difference (LSD) test. A $P < 0.05$ was considered to denote a statistically significant difference.

Results

Contusion concomitant with ischemia injury aggravated muscle necrosis in the early stage

At 24 h postinjury, the muscle fibers in group C were ruptured or partially defective. In group I, the GM was intact but swollen. In group C + I, in addition to being ruptured and swollen, the muscle fibers also appeared partially pale or gray (Figure 1(A)). The wet-to-dry ratios of group I and group C + I were significantly higher than that of group C ($P < 0.001$, Figure 1(B)).

Representative results of TTC staining of the GM are shown in Figure 1(C). Viable fibers were stained a dark purple-red color, and infarcted fibers appeared pale brown or light pink. The ratio of the infarct area to the total area was 0.08 ± 0.07% in the control group, 13.44 ± 2.12% in group C, 5.32 ± 1.14% in group I, and 27.78 ± 7.06% in group C + I.

The infarct area in group C + I was significantly larger than that in group C ($P < 0.001$), group I ($P < 0.001$), and the control group ($P < 0.001$) (Figure 1(D)).

HE staining of the GM was performed to further assess the morphological changes that occurred after injury in each group. Disordered myofibers, swollen intercellular spaces, and ruptured myocytes were discovered at 24 h postinjury (Figure 1(E)). Injured muscle fibers were scattered in group I but more concentrated in group C. The injured muscle fibers were concentrated in the injury area but also appeared at scattered sites distant from the injury site in group C + I. Furthermore, inflammatory cells were found to infiltrate the interfiber space in each group. The muscle injury score of group C + I was 30.38 ± 8.97%, which was significantly higher than that of group C (17.48 ± 4.10%, $P = 0.004$) and group I (4.43 ± 0.69%, $P < 0.001$) (Figure 1(F)).

Contusion concomitant with ischemia injury induced more severe systemic and local reactions

At 24 h postinjury, the serum concentration of CK in group C + I was 2099.74 ± 502.30 U/L, which was significantly higher than that in group C (1455.14 ± 313.36 U/L, $P = 0.03$) and group I (1326.40 ± 242.96 U/L, $P = 0.008$). No significant difference in serum CK concentration was detected between group C and group I (Figure 2(A)). The serum concentration of LDH in group C + I was 3152.50 ± 339.37 U/L, which was significantly higher than that in group I (2034.84 ± 258.44 U/L, $P < 0.001$). No significant difference in serum LDH concentration was detected between group C + I and group C (2611.54 ± 478.31 U/L) or between group I and group C (Figure 2(B)). The muscle TNF-α content in group C + I was 5.51 ± 1.08 pg/mL, which was significantly higher than that in group C (3.36 ± 1.02 pg/mL, $P = 0.008$) and group I (2.78 ± 0.68 pg/mL, $P = 0.001$). No significant difference in muscle TNF-α content was detected between the control (2.48 ± 0.76 pg/mL) and group C or group I (Figure 2(C)).

Furthermore, CMAPs and muscle force were measured at 24 h postinjury to evaluate functional changes (Figure 2(D) to (F)). No obvious CMAPs were detected in group C + I or group I, and the CMAP amplitude in group C (24.46 ± 1.79 mV) was significantly lower than that in the control group (32.97 ± 1.56 mV, $P = 0.009$) (Figure 2(G)). The twitch forces of group C (48.88 ± 1.91 N), group I (37.65 ± 2.68 N), and group C + I (11.89 ± 1.48 N) were significantly lower than that of the control group (61.50 ± 1.24 N), and the twitch force of group C + I was the lowest ($P < 0.001$) (Figure 2(H)). Similarly, the tetanus forces of group C (55.46 ± 6.70 N), group I (37.33 ± 4.26 N), and group C + I (16.69 ± 2.44 N) were significantly lower than that of the control group (78.87 ± 5.35 N), and the tetanus force of group C + I was the lowest ($P < 0.001$) (Figure 2(I)).

Contusion concomitant with ischemia injury aggravated the loss of limb function during the follow-up period

All animals immediately experienced motor dysfunction of the limb to different degrees after injury. Compared with that of the contralateral limb, the gait of the injured hindlimb showed mild claudication in group C, while the flexion and extension of the knee and ankle joints were almost normal. In contrast, the injured hindlimb exhibited obvious gait dysfunction in group I and group C + I. The rats walked with a dragging motion and were unable to flex and extend the knee and ankle joints. The motor function and gait of the injured limbs gradually improved in each group. At 28 days postinjury, no claudication was observed in group C, and the motion of the injured hindlimb was normal. In addition, mild claudication was observed in group I and group C + I. The flexion of the ankle was mildly restricted in group C + I but was normal in group I.

At 28 days postinjury, the appearance of the paws of each rat in the resting (completely anesthetized) state was recorded, and mild paw contracture was observed in group I and group C + I (Figure 3(A)). The GM was then dissected for further assessment. The injured GMs of rats in each injury group showed different degrees of muscle atrophy (Figure 3(B)) compared with those on the contralateral side. The mass ratio of the injured side to the control side in group C + I (0.62 ± 0.05) was significantly lower than that in group C (0.84 ± 0.05; $P < 0.001$) and group I (0.75 ± 0.09; $P < 0.05$) (Figure 3(C)).

CMAPs and muscle force were measured 28 days postinjury (Figure 3(D) to (F)). There was no significant difference in CMAP amplitude between group C (36.36 ± 2.24 mV) and the control (38.43 ± 3.12 mV). Similarly, no significant difference in CMAP amplitude was detected between group I (26.09 ± 1.03 mV) and group C + I (24.09 ± 0.49 mV), and the CMAP amplitude of both of these groups was significantly lower than that of the control group ($P < 0.001$) (Figure 3(G)).

There was no significant difference in twitch force between group I (82.27 ± 3.64 N) and control (86.79 ± 2.57 N). The twitch force of group C (46.45 ± 2.37 N) was lower than that of group I and the control group, and the twitch force of group C + I (24.83 ± 1.35 N) was the lowest ($P < 0.001$) (Figure 3(H)). Similarly, no significant difference in tetanus force was detected between group I (84.56 ± 5.31 N) and control (87.99 ± 5.59 N). The tetanus force of group C (57.73 ± 5.69 N) and group C + I (37.43 ± 1.51 N) was significantly lower than that of the control group, and the tetanus force of group C + I was the lowest ($P < 0.001$) (Figure 3(I)).

Contusion concomitant with ischemia injury hindered muscle fiber regeneration, aggravated muscle fibrosis, and decreased SC differentiation

Masson trichrome staining of GMs was performed at different time points to further evaluate the morphological changes that occurred during the recovery process. At 24 h postinjury, muscle necrosis was observed to different degrees in each group, similar to what was revealed by HE staining. After that, the necrotic areas were gradually replaced with regenerated muscle fibers and fibrous tissue (Figure 4(A), supplemental material Figure 1). At 28 days postinjury, the group C + I demonstrated a higher percentage of 0–600 μm^2 fibers and a lower percentage of 600–1200 μm^2 fibers compared with group C ($P < 0.05$) and group I ($P < 0.05$). The percentage of larger fibers (> 1200 μm^2) in group C + I was lower than in group C ($P < 0.05$) too. The group C + I demonstrated a leftward shift in frequency distribution (toward smaller fiber sizes) when compared with other groups (Figure 4(B)).

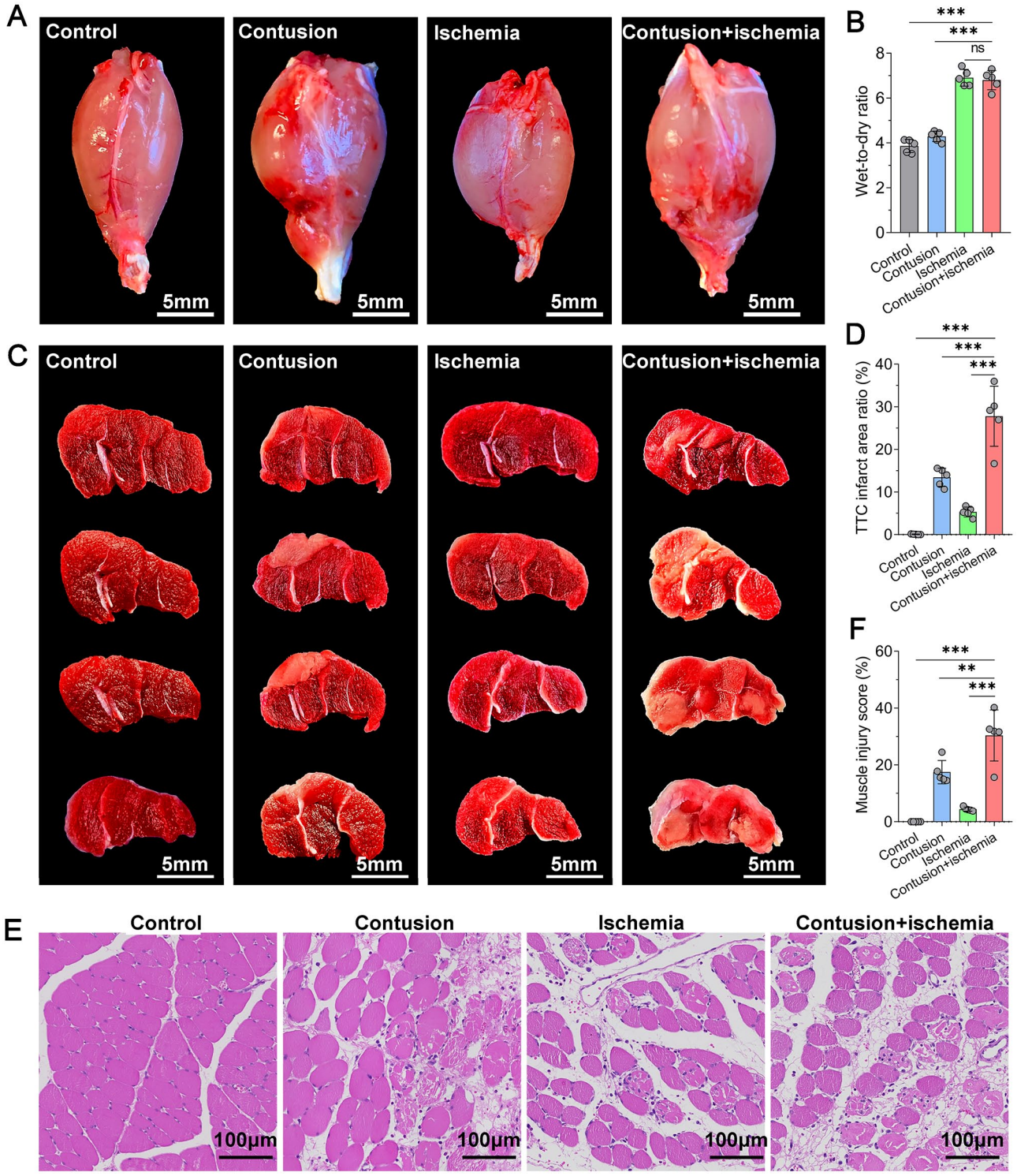

Figure 1. Contusion concomitant with ischemia injury aggravates muscle necrosis at 24 h postinjury. (A) Contusion injury ruptured muscle fibers (arrow), while ischemia injury caused muscle swelling. Contusion concomitant with ischemia injury caused muscle fiber rupture (arrow) and swelling. Bar = 500 mm. (B) Contusion concomitant with ischemia injury and ischemia injury alone caused more significant swelling than contusion injury ($P < 0.001$). (C, D) TTC staining showed that contusion concomitant with ischemia injury resulted in a larger infarct area than contusion injury ($P < 0.001$) and ischemia injury ($P < 0.001$). Bar = 500 mm. (E, F) HE staining of injured GMs from each group. The muscle injury score following contusion concomitant with ischemia injury was higher than that following contusion injury ($P = 0.004$) and following ischemia injury ($P < 0.001$). Bar = 100 μm. All data are presented as the means ± SDs. $n = 5$. ***$P < 0.001$; **$P < 0.01$; *$P < 0.05$; ns: not significant. (A color version of this figure is available in the online journal.)

The fibrotic area in the control group was 1.35 ± 0.71% of the total area, and the fibrotic area in group C + I (15.90 ± 1.48%) was larger than that in group C (10.32 ± 0.71%, $P < 0.001$) and group I (3.11 ± 1.42%. $P < 0.001$) (Figure 4(C)).

Moreover, Sirius red staining of the GM was performed to evaluate the change in collagen content and type in each group (Figure 5(A) and (B)). Under bright field microscopy, collagens constituted 1.40 ± 0.23% of the total area in the

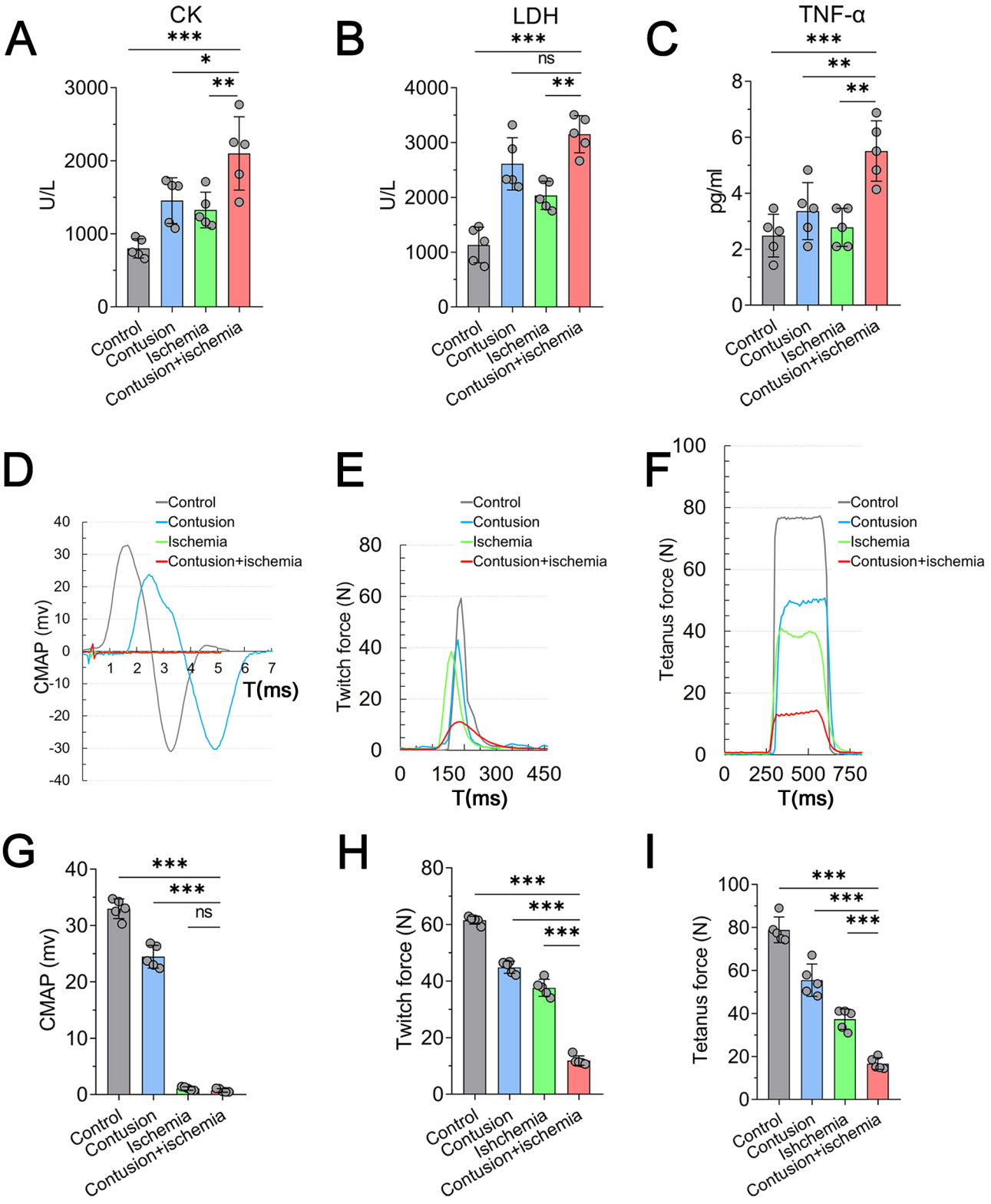

Figure 2. Contusion concomitant with ischemia injury induced more severe systemic and local reactions. (A–C) Contusion concomitant with ischemia injury resulted in higher levels of serum CK and LDH and higher muscle content of TNF-α at 24 h postinjury. (D–F) CMAPs and muscle force at 24 h postinjury. (G) No obvious CMAPs were detected in the contusion concomitant with ischemia injury group or ischemia injury group. (H, I) The twitch force and tetanus force of the GM were the lowest in the contusion concomitant with ischemia injury group ($P < 0.001$) among all groups. All data are presented as the means ± SDs. $n = 5$. ***$P < 0.001$; **$P < 0.01$; *$P < 0.05$; ns: not significant. (A color version of this figure is available in the online journal.)

control group. The proportion of collagen fibers in group C (5.10 ± 2.02%) and group I (2.97 ± 0.72%) were higher than that in the control group (Figure 5(C)). The proportion of collagen fibers in group C + I was 11.61 ± 1.67%, which was significantly higher than that in the other groups ($P < 0.001$) (Figure 5(C)). Two main types of collagens were observed under polarized light in each group. Collagen I appeared red or orange, while collagen III appeared green (Figure 5(B)).

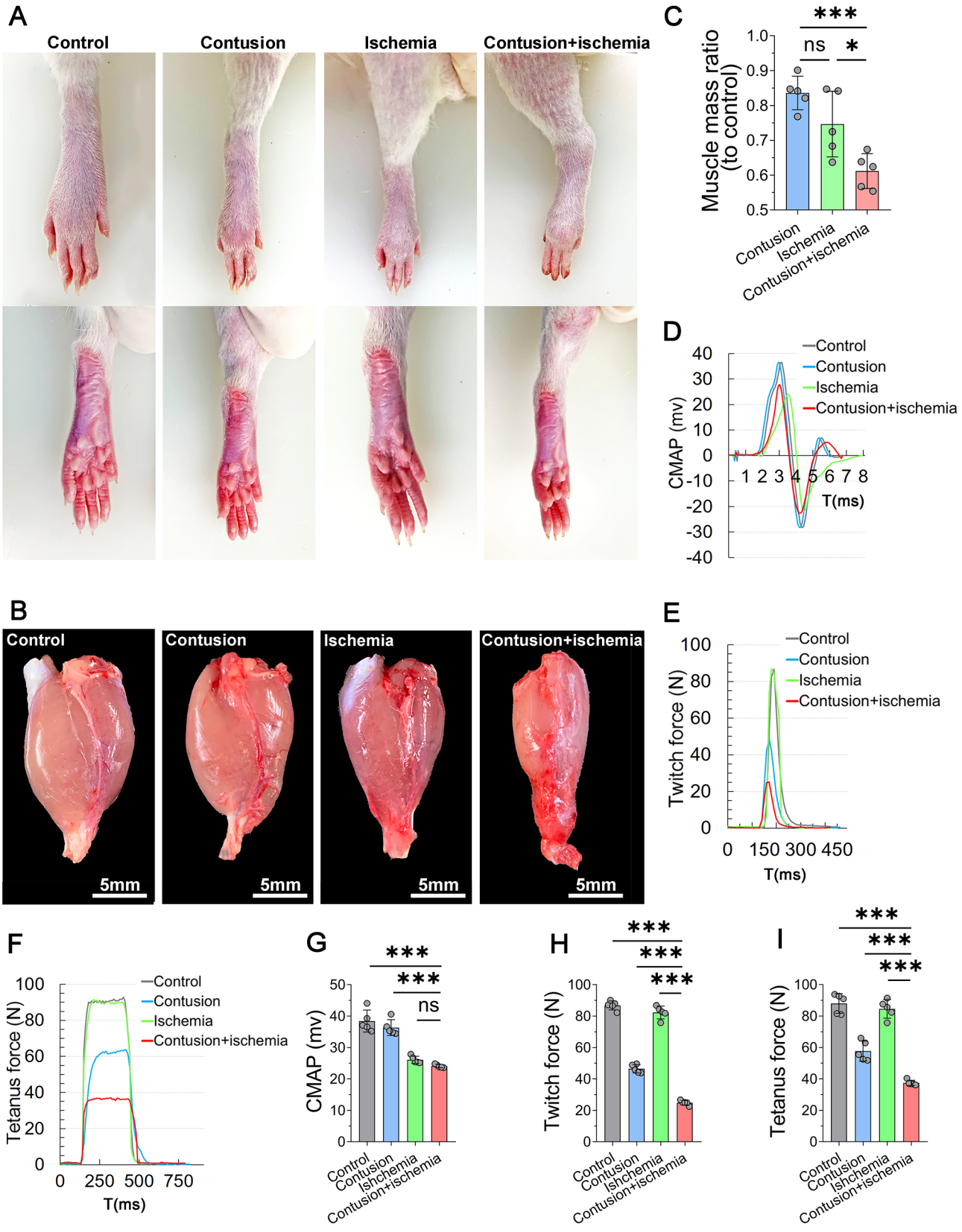

Figure 3. Contusion concomitant with ischemia injury aggravated the loss of limb function during the 28-day follow-up period. (A) Contusion concomitant with ischemia injury and ischemia injury alone induced mild paw contracture at 28 days postinjury. (B, C) Contusion concomitant with ischemia injury caused more significant muscle atrophy in the GM than contusion injury ($P < 0.001$) or ischemia injury ($P < 0.05$). (D–F) CMAPs and muscle force at 28 days postinjury. (G) In the contusion concomitant with ischemia injury group and ischemia injury group, the CMAP amplitude was lower than that in the contusion injury group and control group. (H, I) The twitch force and tetanus force of the GM were the lowest in the contusion concomitant with ischemia injury group ($P < 0.001$) among all groups. All data are presented as the means ± SDs. $n = 5$. ***$P < 0.001$; **$P < 0.01$; *$P < 0.05$; ns: not significant. (A color version of this figure is available in the online journal.)

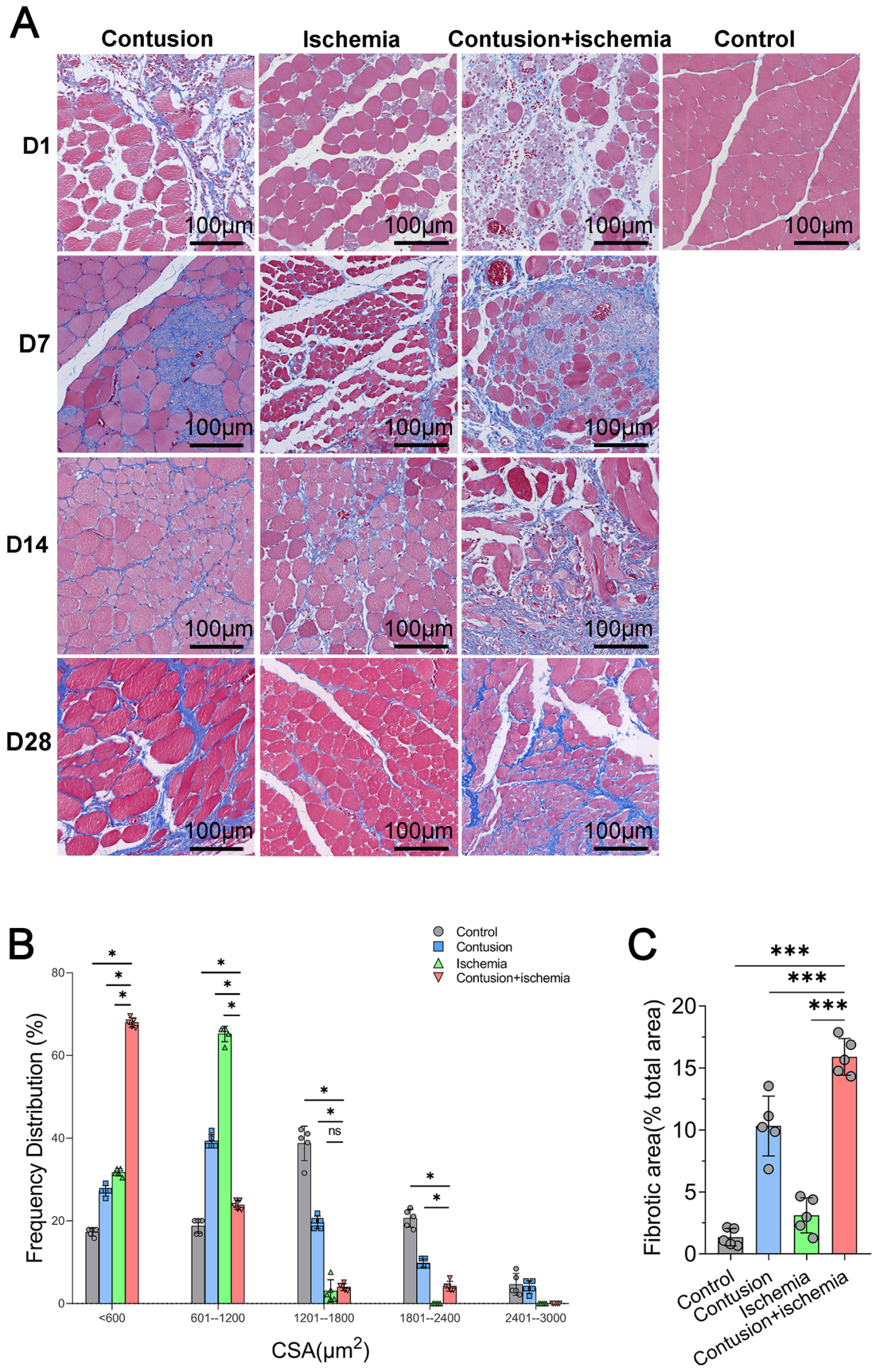

Figure 4. Contusion concomitant with ischemia injury hindered the regeneration of muscle fibers and aggravated muscle fibrosis. (A) Masson trichrome staining of tissues from each group at 1, 7, 14, and 28 days postinjury. (B) At 28 days postinjury, Masson trichrome staining revealed that the group C + I demonstrated a higher percentage of smaller (0–600 μm²) fibers and a lower percentage of larger (600–3000 μm²) fibers compared with group C or group I. (C) At 28 days postinjury, Masson trichrome staining revealed that the fibrotic area was the largest in the contusion concomitant with ischemia injury group. All data are presented as the means ± SDs. $n = 5$. ***$P < 0.001$; **$P < 0.01$; *$P < 0.05$; ns: not significant. (A color version of this figure is available in the online journal.)

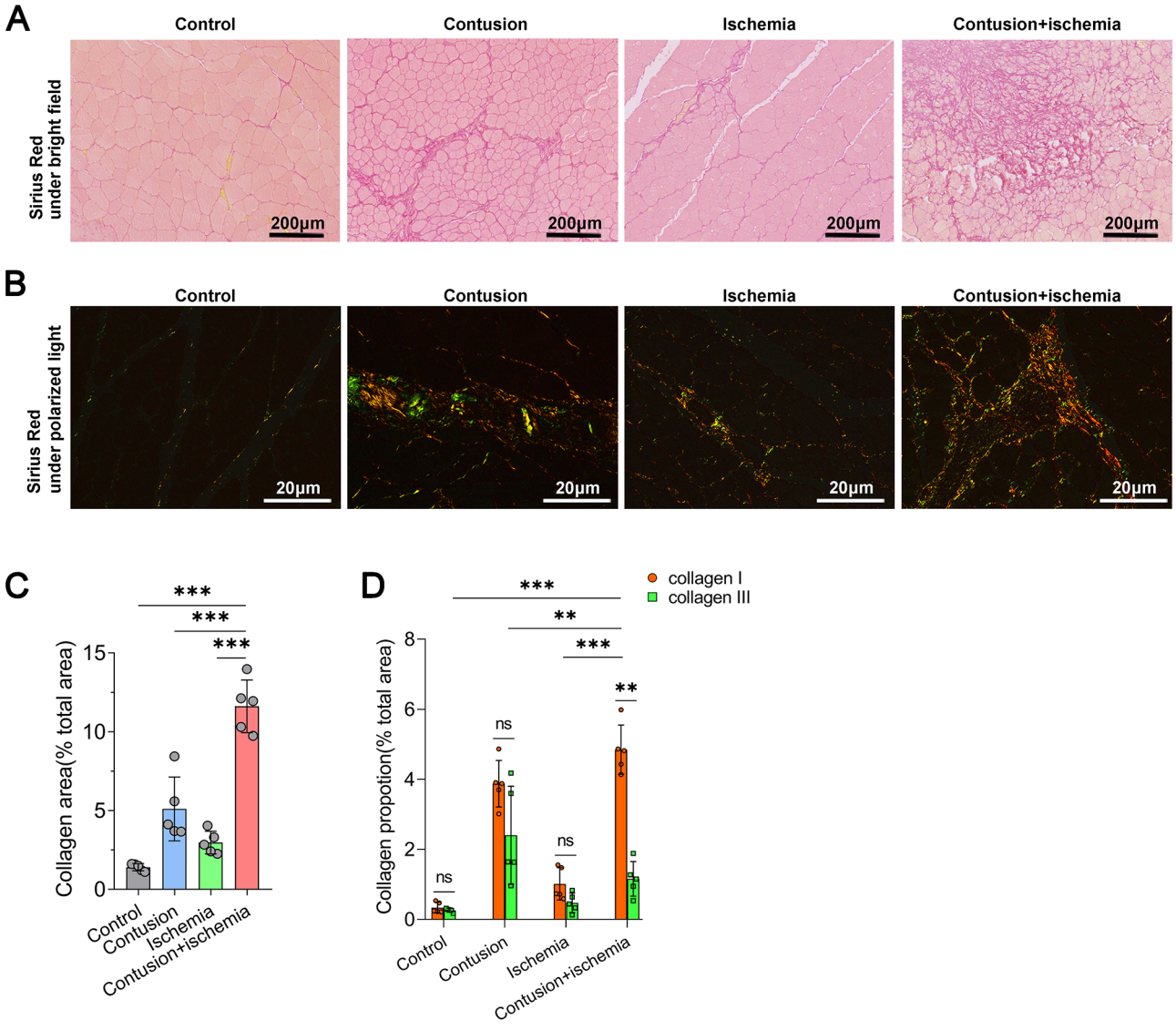

Figure 5. Contusion concomitant with ischemia injury aggravated collagen I deposition. (A, B) Sirius Red staining of GMs from each group at 28 days postinjury, under bright field (A, bar = 200 μm) and polarized light (B, bar = 20 μm), respectively. (C) Under bright field microscopy, the largest number of collagens was observed in the contusion concomitant with ischemia injury group ($P < 0.001$). (D) Under polarized light, more collagen I than collagen III was observed in the contusion concomitant with ischemia injury group ($P < 0.001$) and ischemia injury group ($P = 0.012$). Collagen I content was the highest in the contusion injury concomitant ischemia injury group ($P < 0.001$). All data are presented as the means ± SDs. $n = 5$. ***$P < 0.001$; **$P < 0.01$; *$P < 0.05$; ns: not significant. (A color version of this figure is available in the online journal.)

In the control group, there was no significant difference in the proportion of collagen I (0.34 ± 0.15%) and that of collagen III (0.26 ± 0.06%) ($P = 0.370$). Similarly, no significant difference in the proportion of collagen I and that of collagen III was detected in group C (3.87 ± 0.66% and 2.40 ± 1.40%, respectively, $P = 0.107$). In addition, the proportion of collagen I was greater than that of collagen III in group I (1.01 ± 0.46% and 0.47 ± 0.27%, respectively, $P = 0.012$) and group C + I (4.85 ± 0.70% and 1.16 ± 0.49%, respectively, $P < 0.001$). Furthermore, more collagen I was found in group C + I than in the other groups ($P < 0.001$) (Figure 5(D)).

To explore the reason for the discrepancies in muscle regeneration between groups, the differentiation of satellite cells (SCs) and muscle fiber regeneration were assessed by immunofluorescence staining of $Pax7^+$ and $MyoD^+$ nuclei, as well as the basement membranes of injured muscles, at 7 days postinjury (Figures 6(A) and 7(A)). The quantitative analysis revealed that there were significantly fewer $Pax7^+$ nuclei in group C + I (8.4 ± 2.65/HPF) than in group I (42.4 ± 7.20/HPF, $P < 0.001$). However, no difference in the number of $Pax7^+$ nuclei was detected among group C + I, group C (8.2 ± 2.04/HPF), and the control group (8.0 ± 3.74/HPF) (Figure 6(B)). Furthermore, there were more $MyoD^+$ nuclei in all injured groups than in the control group (5.0 ± 0.89/HPF). There were significantly fewer $MyoD^+$ nuclei in group C + I (12.2 ± 1.83/HPF) than in group C (25.4 ± 3.38/HPF, $P < 0.001$) and group I (65 ± 4.82/HPF, $P < 0.001$) (Figure 7(B)).

Discussion

Contusion concomitant with ischemia injury skeletal muscle is common in clinical practice. Most studies mainly focus

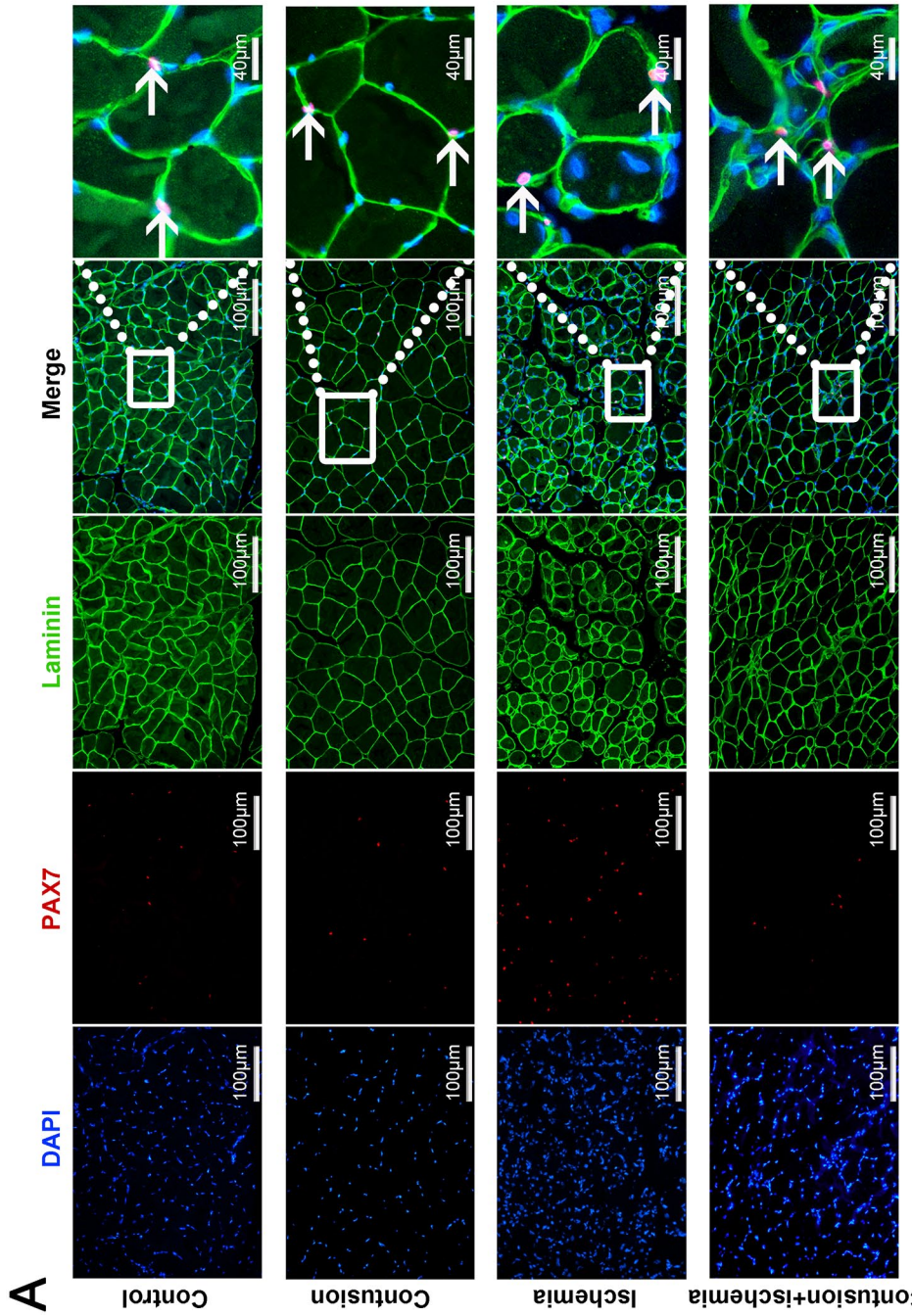

Figure 6. Contusion concomitant with ischemia injury hindered the differentiation of satellite cells (SCs). (A) Immunofluorescence staining of DAPI, $Pax7^+$ SCs, and laminin in the muscle membrane at 7 days postinjury. Bar = 100 μm in columns 1–4; bar = 250 μm in column 5. (B) There were significantly fewer $Pax7^+$ nuclei in the contusion concomitant with ischemia injury group than in the ischemia group ($P < 0.001$). All data are presented as the means ± SDs. $n = 5$. $^{***}P < 0.001$; $^{**}P < 0.01$; $^{*}P < 0.05$; ns: not significant; HPF: high-power fields. (A color version of this figure is available in the online journal.)

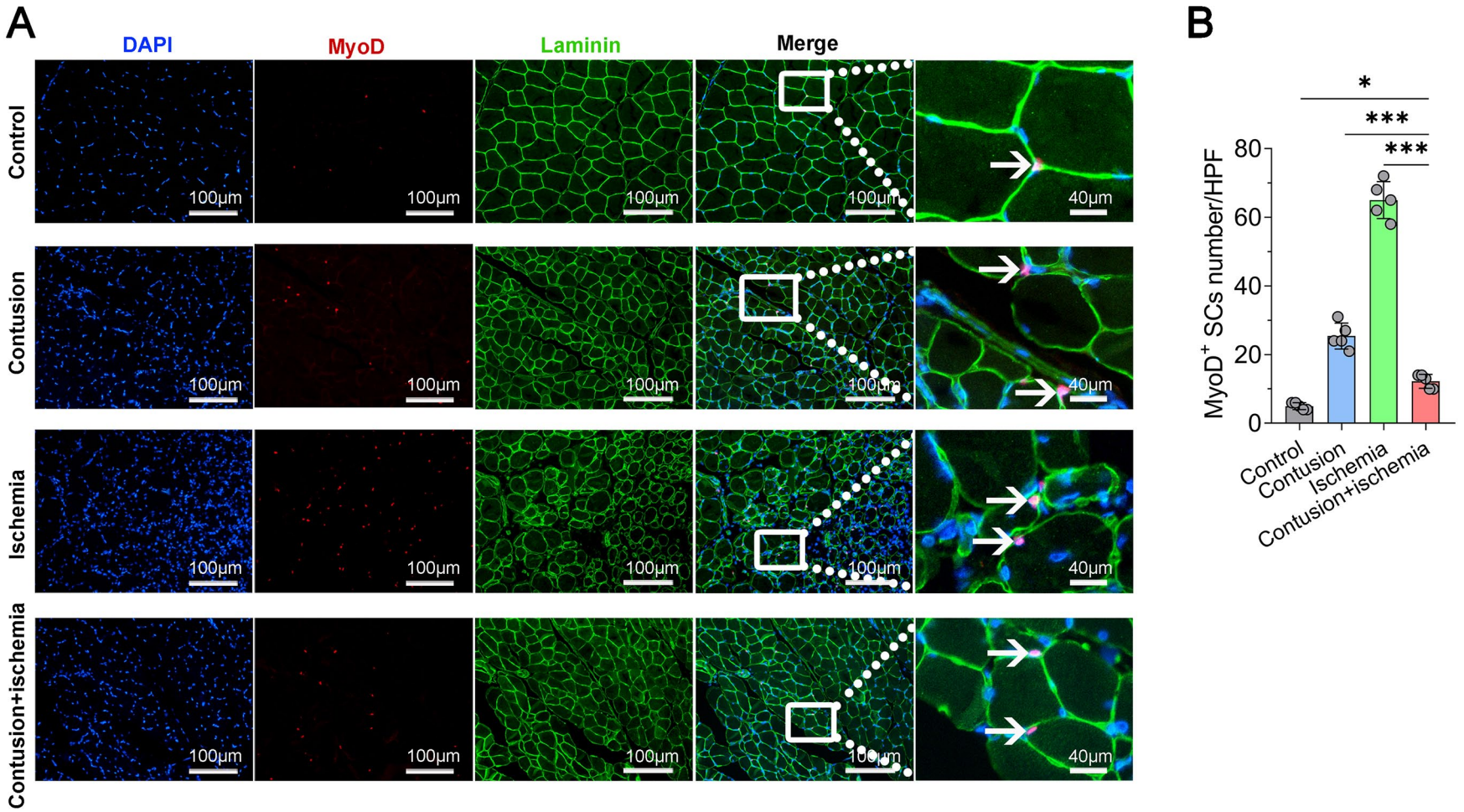

Figure 7. Contusion concomitant with ischemia injury hindered the differentiation of satellite cells (SCs). (A) Immunofluorescence staining of DAPI, MyoD$^+$ SCs, and laminin in the muscle membrane at 7 days postinjury. Bar = 100 μm in columns 1–4; Bar = 250 μm in column 5. (B) There were more MyoD$^+$ nuclei in all injured groups than in the control group. There were significantly fewer MyoD$^+$ nuclei in the contusion concomitant with ischemia injury group than in the contusion injury group ($P < 0.001$) and ischemia injury group ($P < 0.001$). All data are presented as the means ± SDs. $n = 5$. ***$P < 0.001$; **$P < 0.01$; *$P < 0.05$; ns: not significant; HPF: high-power fields. (A color version of this figure is available in the online journal.)

on the outcomes brought by contusion injury or ischemia injury alone. Even though the mechanisms of these injuries are completely different, their associated morphological, metabolic, and biochemical changes, especially those related to the muscle regeneration process, are similar.[21,22] Emerging studies indicate that there are biological overlaps and crosstalk between contusion and ischemia injury in brain[23] and spinal cord.[24] Ghaly and Marsh[25] have demonstrated that the induction of ischemia-induced oxidative stress in skeletal muscle before contusion injury exacerbated the inflammatory response and enhanced fibrotic scar tissue formation. The alterations that occur in skeletal muscle after contusion concomitant with ischemia injury have not been clearly revealed. The results in this study indicated that compared with contusion injury or ischemia injury alone, contusion injury concomitant with ischemia injury not only aggravated early muscle fiber injury but also hindered muscle functional recovery by decreasing the differentiation of SCs and exacerbating fibrosis.

Significant muscle necrosis after contusion injury with concomitant ischemia injury may be due to dysfunction of the inflammatory response

CK and LDH are commonly used biomarkers in detecting muscle injury.[26] In this study, results of CK, LDH, together with HE staining results suggest that contusion injury concomitant with ischemia injury induces more severe muscle necrosis than contusion injury or ischemia injury alone. TNF-α, one of the most common inflammatory factors, plays a role in the release of other cytokines and the recruitment and migration of leukocyte.[27] In this study, higher expression of muscle TNF-α indicates that inflammatory response took place in skeletal muscle after contusion injury concomitant with ischemia injury is more significant than contusion injury or ischemia injury alone. Interestingly, muscle TNF-α level in group I was close to normal at 24 h postinjury, seemingly inconsistent with the HE staining results in this study. One reason may be that TNF-α expression levels are time-dependent, and another reason is that 2 h of ischemia, used in this study caused only minor muscle damage compared with results from other studies.[28,29]

In this study, a decrease in the CMAP amplitude and force production was observed in group I and group C + I at 24 h postinjury, indicating that ischemia causes severe harmful effects on skeletal muscle in the early stage. These findings are compatible with the previous study. Ferry *et al.* evaluated the effects of ischemia on the mechanical activity of the tibialis anterior muscles in the mouse hindlimb. It was found that the tetanic force was significantly lower in ischemia muscles than the control group.[30]

However, different results were discovered in the CMAP amplitude and force production between group C and group I. This is consistent with the results of the HE injury score in this study. The reason may be that the degree of inflammatory response caused by contusion and ischemia is different. On one hand, contusion injury to skeletal muscle not only causes myofiber rupture but also leads to leads to inflammation and oxidative stress. Contusion to skeletal muscle directly ruptures myofibers. And then, neutrophils and macrophages infiltrate into the injury site in response to chemotactic signals and phagocytize the muscle debris.[31] They also simultaneously release inflammatory factors, which cause secondary damage to the surrounding tissue. A recent microarray and bioinformatics analysis indicates that contusion injury to skeletal muscle down-regulates the expression of oxidation- and respiratory complex-related genes, and thus results in impaired mitochondrial respiration and the production of a huge quantity of reactive oxygen species (ROS) at 24–48 h after muscle injury.[1] ROS is the main source of oxidative stress, which can activate several transcription factors and lead to the differential expression of genes involved in inflammatory pathways.[32] On the other hand, ischemia to skeletal muscle induces inflammatory response and oxidative stress radically.[8] First, ischemia induces extensive inflammatory infiltration with robust neutrophil extracellular trap (NET) formation in skeletal muscle.[9] Second, ischemia induces ROS production via the activation of xanthine oxidase (XO) in endothelial cells in skeletal muscle, which could be further exacerbated after reperfusion.[10] Excessive ROS accumulation attacks the membrane lipids, resulting in myofiber ruptures,[33] aggravating inflammations. The above mechanism well illustrates the different phenotype of skeletal muscle necrosis after contusion injury or ischemia injury alone. Although not been clearly explored, we prefer to believe that dysfunction of the inflammatory response leads to significant muscle necrosis after contusion injury concomitant with ischemia injury.

Significant muscle function impairment after contusion concomitant with ischemia injury results from insufficient muscle regeneration and progressive fibrosis

As discussed before, repair of skeletal muscle after injury is a complex and well-understood process that includes the inflammatory response, myofiber regeneration, and remodeling of muscle tissue. Previous studies have demonstrated that although the inflammatory response markedly contributes to secondary damage, it is crucial for the repair of skeletal muscle after injury.[34] In the early Th1 response, for example, TNF-α mediates myeloid cells to stimulate the proliferative of myogenesis.[35] However, persistent or potent inflammation induces excess proliferation and activation of fibroblasts, leading to extensive fibrosis and formation of dense scar tissue.[36] These pathological processes involve the replacement of functional and contractile fibers with rigid scar-like tissue containing extracellular matrix proteins, such as fibronectin, collagens, and proteoglycans,[37] which inhibit the muscle regeneration process and result in incomplete recovery. These findings are consistent with those of our study, which suggest that the more severe inflammatory response in the early stage was related to the formation of more rigid collagen I after contusion concomitant with ischemia injury.

The proliferation and differentiation of SCs dominate the repair process. SCs remain quiescent (in a nondividing state) in uninjured muscle and can be identified by the expression of Pax7.[38] After injury, quiescent SCs become activated and give rise to myogenic progenitors that massively proliferate, differentiate, and fuse to form new myofibers. This process is partially mediated by induced expression of MyoD and

other myogenic regulatory factors (MRFs).[39] Emerging studies have revealed that when activated, SCs undergo asymmetric cell division to generate a stem cell and a proliferative progenitor, which forms new muscle.[40] SCs that do not commit to differentiation can downregulate the expression of MyoD and undergo self-renewing proliferation to replenish the pool of SCs.[41] As introduced in other papers,[42] the expression level of PAX7 was used to indicate increasing supplementation of the SC pool, while the expression level of MyoD was used to suggest increased differentiation and regeneration. The results in this study suggested that fewer SCs committed to differentiation after contusion concomitant with ischemia injury than after contusion injury or ischemia injury alone. This result indicates that muscle regeneration is more defective and fibrosis is more progressive following contusion injury and ischemia injury.

Conclusions

Compared with contusion injury or ischemia injury alone, contusion concomitant with ischemia injury to skeletal muscle aggravates muscle fiber necrosis and the inflammatory response in the early stage after injury. During the skeletal muscle repair process, contusion concomitant with ischemia injury hinders muscle functional recovery by impairing the differentiation of SCs and exacerbating fibrosis. This study improves our understanding of the pathological alterations in skeletal muscle after contusion concomitant with ischemia injury and, provides insight into the potential mechanism of muscle regeneration disorders caused by this type of injury.

AUTHORS' CONTRIBUTIONS

All authors participated in the design, interpretation of the studies and review of the manuscript. PD and SQ conducted the experiments; FL and YJ help to perform the experiments; PD, SQ, and CZ analyzed the data including statistical analysis; PD wrote the manuscript; CZ and QZ conceptualized the idea, initiated the project, provided research support, designed the experiment, and revised the manuscript.

DECLARATION OF CONFLICTING INTERESTS

The author(s) declared no potential conflicts of interest with respect to the research, authorship, and/or publication of this article.

FUNDING

The author(s) disclosed receipt of the following financial support for the research, authorship, and/or publication of this article: This study was financially supported by the National Natural Science Foundation of China (grant no. 82171650) and Guangdong Basic and Applied Basic Research Foundation (no. 2020A1515011143).

ORCID ID

Peijun Deng https://orcid.org/0000-0003-2749-7750

SUPPLEMENTAL MATERIAL

Supplemental material for this article is available online.

REFERENCES

1. Li N, Bai RF, Li C, Dang LH, Du QX, Jin QQ, Cao J, Wang YY, Sun JH. Insight into molecular profile changes after skeletal muscle contusion using microarray and bioinformatics analyses. *Biosci Rep* 2021;**41**:BSR20203699
2. Tidball JG. Mechanisms of muscle injury, repair, and regeneration. *Compr Physiol* 2011;**1**:2029–62
3. Li HY, Zhang QG, Chen JW, Chen SQ, Chen SY. The fibrotic role of phosphatidylinositol-3-kinase/Akt pathway in injured skeletal muscle after acute contusion. *Int J Sports Med* 2013;**34**:789–94
4. Xiao W, Liu Y, Chen P. Macrophage depletion impairs skeletal muscle regeneration: the roles of pro-fibrotic factors, inflammation, and oxidative stress. *Inflammation* 2016;**39**:2016–28
5. Zhao L, Liu X, Zhang J, Dong G, Xiao W, Xu X. Hydrogen sulfide alleviates skeletal muscle fibrosis via attenuating inflammation and oxidative stress. *Front Physiol* 2020;**11**:533690
6. McDermott MM, Ferrucci L, Gonzalez-Freire M, Kosmac K, Leeuwenburgh C, Peterson CA, Saini S, Sufit R. Skeletal muscle pathology in peripheral artery disease: a brief review. *Arterioscler Thromb Vasc Biol* 2020;**40**:2577–85
7. Bagis Z, Ozeren M, Buyukakilli B, Balli E, Yaman S, Yetkin D, Ovla D. Effect of iloprost on contractile impairment and mitochondrial degeneration in ischemia-reperfusion of skeletal muscle. *Physiol Int* 2018;**105**:61–75
8. Paradis S, Charles AL, Meyer A, Lejay A, Scholey JW, Chakfé N, Zoll J, Geny B. Chronology of mitochondrial and cellular events during skeletal muscle ischemia-reperfusion. *Am J Physiol Cell Physiol* 2016;**310**:C968–82
9. Edwards NJ, Hwang C, Marini S, Pagani CA, Spreadborough PJ, Rowe CJ, Yu P, Mei A, Visser N, Li S, Hespe GE, Huber AK, Strong AL, Shelef MA, Knight JS, Davis TA, Levi B. The role of neutrophil extracellular traps and TLR signaling in skeletal muscle ischemia reperfusion injury. *FASEB J* 2020;**34**:15753–70
10. Gillani S, Cao J, Suzuki T, Hak DJ. The effect of ischemia reperfusion injury on skeletal muscle. *Injury* 2012;**43**:670–5
11. Olson SA, Glasgow RR. Acute compartment syndrome in lower extremity musculoskeletal trauma. *J Am Acad Orthop Surg* 2005;**13**:436–44
12. Shadgan B, Reid WD, Harris RL, Jafari S, Powers SK, O'Brien PJ. Hemodynamic and oxidative mechanisms of tourniquet-induced muscle injury: near-infrared spectroscopy for the orthopedics setting. *J Biomed Opt* 2012;**17**:081408-1
13. Yu TS, Cheng ZH, Li LQ, Zhao R, Fan YY, Du Y, Ma WX, Guan DW. The cannabinoid receptor type 2 is time-dependently expressed during skeletal muscle wound healing in rats. *Int J Legal Med* 2010;**124**:397–404
14. Fan YY, Ye GH, Lin KZ, Yu LS, Wu SZ, Dong MW, Han JG, Feng XP, Li XB. Time-dependent expression and distribution of Egr-1 during skeletal muscle wound healing in rats. *J Mol Histol* 2013;**44**:75–81
15. Atahan E, Ergün Y, Kurutaş EB, Alici T. Protective effect of zinc aspartate on long-term ischemia-reperfusion injury in rat skeletal muscle. *Biol Trace Elem Res* 2010;**137**:206–15
16. Pekoglu E, Buyukakilli B, Turkseven CH, Balli E, Bayrak G, Cimen B, Balci S. Effects of trans-cinnamaldehyde on reperfused ischemic skeletal muscle and the relationship to laminin. *J Invest Surg* 2021;**34**:1329–1338
17. Bederson JB, Pitts LH, Germano SM, Nishimura MC, Davis RL, Bartkowski HM. Evaluation of 2,3,5-triphenyltetrazolium chloride as a stain for detection and quantification of experimental cerebral infarction in rats. *Stroke* 1986;**17**:1304–8
18. McCormack MC, Kwon E, Eberlin KR, Randolph M, Friend DS, Thomas AC, Watkins MT, Austen WG Jr. Development of reproducible histologic injury severity scores: skeletal muscle reperfusion injury. *Surgery* 2008;**143**:126–33
19. Mintz EL, Passipieri JA, Franklin IR, Toscano VM, Afferton EC, Sharma PR, Christ GJ. Long-term evaluation of functional outcomes following rat volumetric muscle loss injury and repair. *Tissue Eng Part A* 2020;**26**:140–56

20. Dyer SE, Remer JD, Hannifin KE, Hombal A, Wenke JC, Walters TJ, Christ GJ. Administration of particulate oxygen generators improves skeletal muscle contractile function after ischemia-reperfusion injury in the rat hindlimb. *J Appl Physiol* 2022;**132**:541–52
21. Moyer AL, Wagner KR. Regeneration versus fibrosis in skeletal muscle. *Curr Opin Rheumatol* 2011;**23**:568–73
22. Tomazoni SS, Frigo L, Dos Reis Ferreira TC, Casalechi HL, Teixeira S, de Almeida P, Muscara MN, Marcos RL, Serra AJ, de Carvalho PTC, Leal-Junior ECP. Effects of photobiomodulation therapy and topical non-steroidal anti-inflammatory drug on skeletal muscle injury induced by contusion in rats-part 2: biochemical aspects. *Lasers Med Sci* 2017;**32**:1879–87
23. Harish G, Mahadevan A, Pruthi N, Sreenivasamurthy SK, Puttamallesh VN, Keshava Prasad TS, Shankar SK, Srinivas Bharath MM. Characterization of traumatic brain injury in human brains reveals distinct cellular and molecular changes in contusion and pericontusion. *J Neurochem* 2015;**134**:156–72
24. Brown A, Nabel A, Oh W, Etlinger JD, Zeman RJ. Perfusion imaging of spinal cord contusion: injury-induced blockade and partial reversal by β2-agonist treatment in rats. *J Neurosurg Spine* 2014;**20**:164–71
25. Ghaly A, Marsh DR. Ischaemia-reperfusion modulates inflammation and fibrosis of skeletal muscle after contusion injury. *Int J Exp Pathol* 2010;**91**:244–55
26. Hsu YJ, Ho CS, Lee MC, Ho CS, Huang CC, Kan NW. Protective effects of resveratrol supplementation on contusion induced muscle injury. *Int J Med Sci* 2020;**17**:53–62
27. Tsivitse SK, Mylona E, Peterson JM, Gunning WT, Pizza FX. Mechanical loading and injury induce human myotubes to release neutrophil chemoattractants. *Am J Physiol Cell Physiol* 2005;**288**:C721–9
28. Gute DC, Ishida T, Yarimizu K, Korthuis RJ. Inflammatory responses to ischemia and reperfusion in skeletal muscle. *Mol Cell Biochem* 1998;**179**:169–87
29. Avci G, Kadioglu H, Sehirli AO, Bozkurt S, Guclu O, Arslan E, Muratli SK. Curcumin protects against ischemia/reperfusion injury in rat skeletal muscle. *J Surg Res* 2012;**172**:e39–46
30. Vignaud A, Hourde C, Medja F, Agbulut O, Butler-Browne G, Ferry A. Impaired skeletal muscle repair after ischemia-reperfusion injury in mice. *J Biomed Biotechnol* 2010;**2010**:724914
31. Chazaud B. Inflammation and skeletal muscle regeneration: leave it to the macrophages! *Trends Immunol* 2020;**41**:481–92
32. Hussain T, Tan B, Yin Y, Blachier F, Tossou MC, Rahu N. Oxidative stress and inflammation: what polyphenols can do for us? *Oxid Med Cell Longev* 2016;**2016**:7432797
33. Watanabe M, Kamimura N, Iuchi K, Nishimaki K, Yokota T, Ogawa R, Ohta S. Protective effect of hydrogen gas inhalation on muscular damage using a mouse hindlimb ischemia-reperfusion injury model. *Plast Reconstr Surg* 2017;**140**:1195–206
34. George C, Smith C, Isaacs AW, Huisamen B. Chronic Prosopis glandulosa treatment blunts neutrophil infiltration and enhances muscle repair after contusion injury. *Nutrients* 2015;**7**:815–30
35. Tidball JG, Villalta SA. Regulatory interactions between muscle and the immune system during muscle regeneration. *Am J Physiol Regul Integr Comp Physiol* 2010;**298**:R1173–87
36. Smith LR, Barton ER. Regulation of fibrosis in muscular dystrophy. *Matrix Biol* 2018;**68–69**:602–15
37. Mahdy MAA. Skeletal muscle fibrosis: an overview. *Cell Tissue Res* 2019;**375**:575–88
38. Malatesta M, Costanzo M, Cisterna B, Zancanaro C. Satellite cells in skeletal muscle of the hibernating dormouse, a natural model of quiescence and re-activation: focus on the cell nucleus. *Cells* 2020;**9**:1050
39. Almada AE, Wagers AJ. Molecular circuitry of stem cell fate in skeletal muscle regeneration, ageing and disease. *Nat Rev Mol Cell Biol* 2016;**17**:267–79
40. Feige P, Brun CE, Ritso M, Rudnicki MA. Orienting muscle stem cells for regeneration in homeostasis, aging, and disease. *Cell Stem Cell* 2018;**23**:653–64
41. Boyer O, Butler-Browne G, Chinoy H, Cossu G, Galli F, Lilleker JB, Magli A, Mouly V, Perlingeiro RCR, Previtali SC, Sampaolesi M, Smeets H, Schoewel-Wolf V, Spuler S, Torrente Y, Van Tienen F, Study Group. Myogenic cell transplantation in genetic and acquired diseases of skeletal muscle. *Front Genet* 2021;**12**:702547
42. Tsuchiya Y, Kitajima Y, Masumoto H, Ono Y. Damaged myofiber-derived metabolic enzymes act as activators of muscle satellite cells. *Stem Cell Reports* 2020;**15**:926–40

(Received October 29, 2021, Accepted April 20, 2022)